

Unifying ultrafast demagnetization and intrinsic Gilbert damping in Co/Ni bilayers with electronic relaxation near the Fermi surface

Wei Zhang,^{1,2} Wei He,^{1,*} Xiang-Qun Zhang,¹ Zhao-Hua Cheng,^{1,2,†} Jiao Teng,³ and Manfred Fähnle⁴

¹State Key Laboratory of Magnetism and Beijing National Laboratory for Condensed Matter Physics, Institute of Physics, Chinese Academy of Sciences, Beijing 100190, People's Republic of China

²School of Physical Sciences, University of Chinese Academy of Sciences, Beijing 100049, China

³Department of Materials Physics and Chemistry, University of Science and Technology Beijing, Beijing 100083, People's Republic of China

⁴Max Planck Institute for Intelligent Systems, Heisenbergstrabe 3, 70569 Stuttgart, Germany

(Received 3 August 2017; published 29 December 2017)

The ability to controllably manipulate the laser-induced ultrafast magnetic dynamics is a prerequisite for future high-speed spintronic devices. The optimization of devices requires the controllability of the ultrafast demagnetization time τ_M and intrinsic Gilbert damping α_{intr} . In previous attempts to establish a relationship between τ_M and α_{intr} , the rare-earth doping of a permalloy film with two different demagnetization mechanisms was not a suitable candidate. Here, we choose Co/Ni bilayers to investigate the relations between τ_M and α_{intr} by means of the time-resolved magneto-optical Kerr effect (TR-MOKE) via adjusting the thickness of the Ni layers, and obtain an approximately proportional relation between these two parameters. The remarkable agreement between the TR-MOKE experiment and the prediction of a breathing Fermi-surface model confirms that a large Elliott-Yafet spin-mixing parameter b^2 is relevant to the strong spin-orbital coupling at the Co/Ni interface. More importantly, a proportional relation between τ_M and α_{intr} in such metallic films or heterostructures with electronic relaxation near the Fermi surface suggests the local spin-flip scattering dominates the mechanism of ultrafast demagnetization, otherwise the spin-current mechanism dominates. It is an effective method to distinguish the dominant contributions to ultrafast magnetic quenching in metallic heterostructures by simultaneously investigating both the ultrafast demagnetization time and Gilbert damping. Our work can open an avenue to manipulate the magnitude and efficiency of terahertz emission in metallic heterostructures such as perpendicular magnetic anisotropic Ta/Pt/Co/Ni/Pt/Ta multilayers, and then it has an immediate implication for the design of high-frequency spintronic devices.

DOI: [10.1103/PhysRevB.96.220415](https://doi.org/10.1103/PhysRevB.96.220415)

Since the pioneering work on the ultrafast demagnetization of a Ni thin film after femtosecond laser irradiation was demonstrated in 1996 by Beaurepaire *et al.* [1], the quest for the ultrafast modification of the magnetic moments has triggered a new field of research, called femtomagnetism. It leads to the dawn of a new era for breaking the ultimate physical limit for the speed of magnetic switching and manipulation, which is relevant to current and future information storage. In the past two decades, ultrafast dynamics in hundreds of femtoseconds has been probed with a femtosecond laser pulse using the magneto-optical Kerr [1] or Faraday effect [2], or other time-resolved techniques such as the high-harmonic generation (HHG) of extreme ultraviolet (XUV) radiation [3], magnetic circular dichroism [4], or spin-resolved two-photon photoemission [5].

Nevertheless, the microscopic mechanism underlying the ultrafast quenching of magnetization remains elusive. Various mechanisms including electron-phonon mediated spin-flip scattering [6–9], electron-electron scattering [10,11], electron-magnon scattering [12,13], direct angular momentum transfer from the photon to electron mediated by spin-orbit coupling [14,15], and coherent interaction among spin electrons and

photons [16], were proposed to explain the ultrafast spin dynamics. In addition, since Malinowski *et al.* [17] first proposed that laser-excited spin-current transport could increase and speed up magnetic quenching in metallic heterostructures, the laser-induced superdiffusive spin current was elevated to play an important role in determining the ultrafast demagnetization in metallic films or heterostructures [18–22]. However, a recent demonstration [23] showed that unpolarized hot electron transport can demagnetize a ferromagnet, indicating that local spin angular momentum dissipation is unavoidable even when superdiffusive spin transport dominates in metallic heterostructures. Moreover, even in similar samples, local spin-flip scattering and nonlocal spin transport mechanisms were proposed respectively by different experimental tools [19,24] to explain ultrafast demagnetization. It is risky for clarifying the underlying ultrafast demagnetization mechanism in such metallic heterostructures. Therefore, an effective method to distinguish the two dominant contributions to ultrafast demagnetization in metallic heterostructures is highly desirable [19,23,24]. Here, we propose that simultaneously investigating both the ultrafast demagnetization time and Gilbert damping [25] is a candidate method, although the relationship between the two parameters has yet to be unified successfully between the experiments and theoretical predictions.

An inverse relation between τ_M and α_{intr} was first derived by Koopmans *et al.* from a quantum-mechanical calculation on the basis of the Elliott-Yafet (EY) spin-flip scattering model [6]. Later, experiments were carried out to demonstrate

*Author to whom correspondence should be addressed: zhcheng@iphy.ac.cn

†Author to whom correspondence should be addressed: hwei@iphy.ac.cn

the prediction in rare-earth-doped permalloy [26,27] and amorphous TbFeCo films [28]. In this case, localized $4f$ electrons rather than itinerant $5d6s$ electrons dominated most of the large magnetic moment in rare-earth elements. Because the $4f$ electrons are far from the Fermi level, their ultrafast demagnetization processes are mediated by $5d6s$ electrons after laser pulse excitation [7]. The indirect excitation leads to the so-called type-II ultrafast demagnetization behavior in rare-earth elements, which is much slower than that of itinerant electrons. Therefore, it is not unexpected that the ultrafast demagnetization time τ_M of permalloy increases with the increasing doping contents of rare-earth elements. Meanwhile, it happened that the Gilbert damping constant of permalloy was also increased by doping $4f$ elements, which mainly comes from the so-called “slow relaxing impurity mechanism” [29]. Therefore, by unavoidably introducing an extra mechanism, a trivial consequence was obtained that the ultrafast demagnetization time τ_M increases as the Gilbert damping α increases in rare-earth-doped permalloy [26]. In hindsight, from this experiment, one cannot confirm the relation between the ultrafast demagnetization time τ_M and Gilbert damping α due to the defects of the experimental design. A genuine relation between the ultrafast demagnetization time and Gilbert damping should be explored in a clean system without an extra demagnetization mechanism. So far, the explicit relationship between the two parameters has yet to be unified successfully between the experiments and theoretical predictions. Our work in Co/Ni bilayers with the electrons relaxing at the Fermi surface can fill in the blank.

In the case of pure $3d$ itinerant electrons relaxing near the Fermi surface after laser excitation, both ultrafast demagnetization and Gilbert damping are determined by the spin-flip scattering of itinerant electrons at the quasiparticles or impurities. Based on the breathing Fermi-surface model of Gilbert damping and on the EY relation for the spin-relaxation time, a proportional relation between τ_M and α_{intr} was derived by Fähnle *et al.* [30,31] for the materials with conductivitylike damping. An inverse relation was also derived which is similar to that proposed by Koopmans *et al.* when resistivity-type damping is dominant in the materials. Although the predicted single numerical values of $\alpha_{\text{intr}}/\tau_M$ are in good agreement with the experimental ones for Fe, Ni, or Co, for a confirmation of the explicit relation between τ_M and α_{intr} , one has to vary the values on the two parameters systematically for one system, as we do here by changing the thickness of the films.

Co/Ni bilayers with a stack of Ta(3 nm)/Pt(2 nm)/Co(0.8 nm)/Ni(d_{Ni} nm)/Pt(1 nm)/Ta(3 nm) were grown on glass substrates by dc magnetron sputtering [32,33]. The thickness of the Ni layer changed from $d_{\text{Ni}} = 0.4$ to 2.0 nm. Their static properties are shown in Part I of the Supplemental Material [34]. Both τ_M and α_{intr} for Co/Ni bilayer systems have been achieved by using the time-resolved magneto-optical Kerr effect (TR-MOKE) technique [21,35]. The reasons for selecting Co/Ni bilayers are threefold. First, Co/Ni bilayers with perpendicular magnetic anisotropy (PMA) are one of the candidates for perpendicular magnetic recording (PMR) media and spintronic devices [36–39]. Second, the electrons in both Co and Ni are itinerant near the Fermi surface and they have the same order of magnitude of demagnetization time [7,10]. Without rare-earth element doping in $3d$ metals, one

can exclude the possibility of an extra slow demagnetization accompanied by doping with $4f$ rare-earth metals. Third, both τ_M and α_{intr} in Co/Ni bilayers can be tuned by changing the Ni thickness. Therefore, Co/Ni bilayers provide an ideal system to investigate the relation between τ_M and α_{intr} . A nearly proportional relationship between τ_M and α_{intr} was evident in Co/Ni bilayers, suggesting that conductivitylike damping [30,31] plays a dominant role. It is distinct in physics with previous experiments [26] where seemingly similar results have been obtained via introducing an extra slow demagnetization mechanism. Moreover, we discussed the origin of Gilbert damping, analyzed its influence on the relation between τ_M and α_{intr} , and proposed a different approach to distinguish the intrinsic spin-flip and extrinsic spin-current mechanisms for ultrafast demagnetization in metallic heterostructures. The finding for this unification can provide a possibility for manipulating laser-induced ultrafast demagnetization via Gilbert damping in high-frequency or ultrafast spintronic devices such as terahertz emitters.

Figure 1(a) shows TR-MOKE signals [40] for films with various Ni layer thicknesses measured with an external field $H = 4000$ Oe. The quantitative values of the intrinsic Gilbert damping constant [41–44] in Fig. 1(b) can be obtained by eliminating the extrinsic contributions (see Part II in the Supplemental Material [34] for details). It was observed that α_{intr} decreases with increasing Ni layer thickness. On the one hand, previous investigations [39,45] have reported that the large PMA originates from the strong spin-orbit coupling effect at the Co/Ni interface. A thickness modification in the Co/Ni bilayer can change the competition between the interface and volume effect, and consequently the PMA. When we plotted the intrinsic Gilbert damping constant as a function of effective anisotropy field (see Fig. 4, Part II in the Supplemental Material [34] for details), a proportional relation was confirmed in our Co/Ni bilayer system, which demonstrates that spin-orbit coupling contributes to both Gilbert damping and PMA (also, for the achievement of an effective anisotropy field, please see Part II in the Supplemental Material [34] for details). On the other hand, the interface between Ni and Pt maybe also modified via changing the Ni layer thickness. Because Gilbert damping increases linearly when the Ni layer becomes thinner, it seems that spin-current dissipation is partly involved. A similar trend was observed in a Pt/CoFeB/Pt system [46], in which a pure nonlocal spin pumping effect dominated the Gilbert damping. Therefore, the total Gilbert damping is equal to $\alpha = \alpha_{\text{intr}} + \alpha_{\text{sp}}$, in which α_{sp} represents the contributions from the spin current. Due to the low spin-diffusion length of Pt, the magnetization precession in the Ni layer entering the Pt layer would be absorbed completely as in a system of Py/Pt, Py/Pd [47], and so on. However, we have to address that, in the case of a variation of ferromagnetic (FM) layer thickness, the amount of spin current pumped out of the ferromagnet is determined entirely by the parameter of interfacial mixing conductance $G_{\text{eff}}^{\text{mix}}$ [48,49]. It is a constant value once the normal metal (NM) thickness is fixed, although Gilbert damping in thinner magnetic layers is enhanced. Therefore, given that the spin current contributes partly to Gilbert damping at present, the spin angular momentum transferring from the Ni layer to the

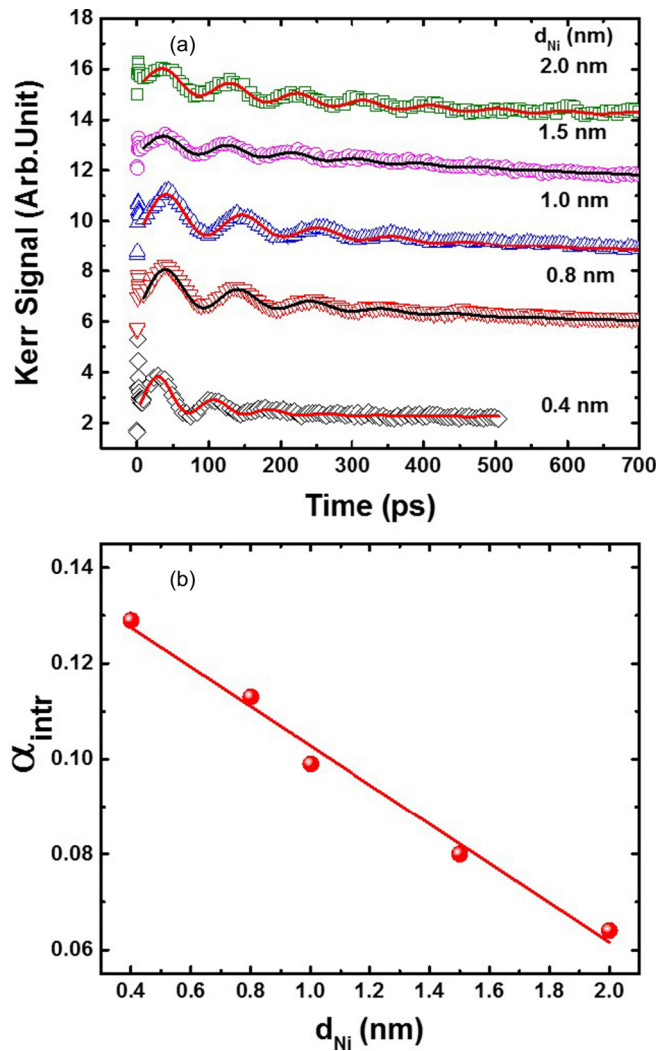


FIG. 1. Spin precession. (a)TR-MOKE signals of Co/Ni bilayers with $d_{Ni} = 0.4 - 2.0$ nm in an applied field $H = 4000$ Oe. (b) Intrinsic Gilbert damping constant as a function of d_{Ni} .

Pt layer would be the same for various Ni layer thicknesses. These discussions hold for another interface between Co and Pt at which the spin angular momentum is dissipated by spin pumping, let alone that both the thicknesses of Co and Pt are the constant values.

The central strategy of our study is to establish a direct correlation between ultrafast demagnetization time and the intrinsic Gilbert damping constant. The intrinsic Gilbert damping constant was extracted from magnetization precession in a time scale of hundreds of ps. Laser-induced ultrafast demagnetization dynamics has been measured carefully within a time delay of 2.5 ps at a step of 15 fs, and a low laser fluence of 1 mJ/cm² was used. Figure 2(a) shows the TR-MOKE signals of the ultrafast demagnetization evolution after optical excitation. A rapid decrease of magnetization takes place on the subpicosecond time scale, followed by a pronounced recovery. As can be seen in this figure, the ultrafast demagnetization rate is altered by changing the Ni thickness.

To identify the effect of heat transport across the film thickness on demagnetization time, a numerical simulation

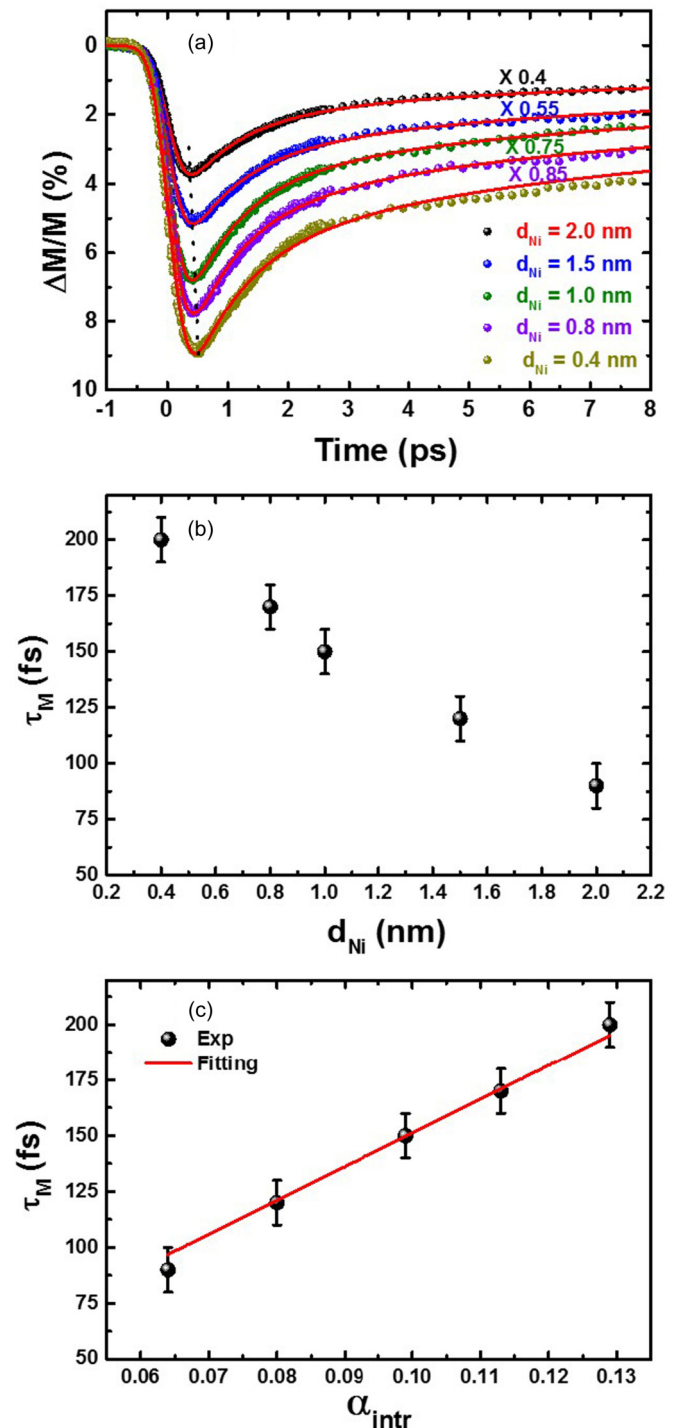


FIG. 2. Ultrafast demagnetization. (a) Ultrafast demagnetization curves with various Ni layer thicknesses. (b) Ultrafast demagnetization time as a function of Ni layer thickness. (c) Ultrafast demagnetization time as a function of Gilbert damping constant. The solid red line indicates the theoretical fitting.

[50] was carried out to demonstrate that the demagnetization time variation induced with thicknesses ranging from 1.2 to 2.8 nm is so small that it can be ignored (see Part II in the Supplemental Material [34] for details), although a relatively large error of τ_M could result when the sample thickness spans are very large. According to the simulation

results, the heat transport not only affects the rate of ultrafast magnetization loss but also the maximum magnetic quenching. So, in the experiment we obtained an ultrafast demagnetization time for various samples with almost the same maximum quenching of 9% to suppress the influence of heat transport [7,21,51–54] as well as the nonlocal spin-current effect [17]. The temporal evolution of magnetization in the subpicosecond time scale was fitted by the analytic solution based on the phenomenological three-temperature model (3TM) [1,17],

$$-\frac{\Delta M(t)}{M} = \left\{ \left[\frac{A_1}{(t/\tau_0 + 1)^{0.5}} - \frac{(A_2\tau_E - A_1\tau_M)}{\tau_E - \tau_M} e^{-\frac{t}{\tau_M}} - \frac{\tau_E(A_1 - A_2)}{\tau_E - \tau_M} e^{-\frac{t}{\tau_M}} \right] \Theta(t) + A_3\delta(t) \right\} * G(t, \tau_G), \quad (1)$$

where $*G(t, \tau_G)$ presents the convolution product with the Gaussian laser pulse profile, whose full width at half maximum (FWHM) is t_G . A temporal stretching of the laser pulse was introduced by the excited hot electrons [55], which is the trigger for the observed ultrafast demagnetization. In the fitting procedure, the demagnetization time τ_M we cared about can be influenced by the value of t_G , which is interdependent with τ_M within the three-temperature model. As is shown in Table I, Part IV in the Supplemental Material [34], t_G was fixed at 330 fs for various samples to eliminate its relevance with τ_M . The time variable in Eq. (1) corresponds to $t = t_{\text{expt}} - t_0$, with t_0 the free fit parameter characterizing the onset of the demagnetization dynamics of the actual data trace, which is fixed at 100 fs for various samples. $\Theta(t)$ is a step function, $\delta(t)$ is the Dirac delta function, and A_1, A_2, A_3 are the fitting constants. The two critical time parameters τ_M, τ_E are the ultrafast demagnetization time and magnetization recovery time, respectively. The well-fitted curves by 3TM are also shown as solid lines in Fig. 2(a), from which the ultrafast demagnetization time τ_M and the magnetization recovery time τ_E were evaluated. Within the 3TM model, the magnetization recovery process is affected by τ_E , characterizing the electron-phonon relaxation, and τ_0 , representing heat transport time scale through the substrates as well as demagnetization time τ_M . In the fitting procedure by the 3TM model, we assigned a fixed value to τ_E , and τ_0 varied slightly to exclude the heat transport effect through thickness. Via changing the single parameter τ_M , we can accurately reproduce the experimental results for various samples. The heat transport across the thickness domains within the 3TM model is characterized by the parameter of τ_0 , which is shown in Table I, Part IV of the Supplemental Material [34] as around 2 ps. It is about three times larger than τ_E , indicating that we are not mixing the heat transport and the electron-phonon relaxation [56]. Both values of τ_E and τ_M are genuine only in this case. Here, the value of τ_0 indicates that the heat was transferred through the substrate in less than 3 ps, rather than what was observed by Busse *et al.* [57] where the heat was trapped laterally in the Gaussian profile up to 1 ns. Therefore, the lateral heat transport effect can be ignored, and hence the modification of precessional dynamics here. As illustrated in Fig. 2(b), it can be clearly seen that τ_M decreases with increasing d_{Ni} .

By replotting Figs. 1(b) and 2(b), an approximately proportional relationship between τ_M and α_{intr} was confirmed by our experimental results [Fig. 2(c)]. This relationship between α_{intr} and τ_M is consistent with the theoretical prediction $\tau_M \propto \alpha_{\text{intr}}$ based on the breathing Fermi-surface model [30,31,58] for materials with conductivitylike damping contributions. On the basis of the breathing Fermi-surface model, the Elliott-Yafet spin-mixing parameter b^2 in Co/Ni bilayers can be estimated from the theoretical equation [30,31], shown as the red solid line in Fig. 2(c),

$$\tau_M = \frac{M}{\gamma F_{\text{el}} p b^2} \alpha, \quad (2)$$

where the quantity contains the derivatives of the single-electron energies with respect to the orientation \mathbf{e} of the magnetization $\mathbf{M} = M\mathbf{e}$. p is a material-specific parameter which should be close to 4. If we use $F_{\text{el}} = 1.87 \times 10^{-23}$ J from an *ab initio* density functional electron theory calculation for fcc bulk Ni [31], the experimental value of the Elliott-Yafet spin-mixing parameter $b^2 = 0.28$ can be estimated in Co/Ni bilayers, which is far larger than that of Co or Ni. The significant enhancement of spin-mixing parameters is related to the strong spin-orbital coupling at the Co/Ni interface since b^2 is proportional to ξ^2 in first-order perturbation theory, where ξ is the coefficient of the spin-orbit coupling. A detailed *ab initio* calculation for the Elliott-Yafet spin-mixing parameter in Co/Ni bilayers is highly desirable. For a derivation of Eq. (2) it must be assumed that the same types of spin-flip scattering processes are relevant for ultrafast demagnetization and damping. The assumption does not say anything about these detailed types. It has been shown in Ref. [9] that mere electron-phonon scattering cannot explain the experimentally observed demagnetization quantitatively. In reality, there are also contributions from electron-electron scattering [11], electron-magnon scattering [12], and from a combination of electron-phonon and electron-magnon scattering [13]. Because, for both demagnetization and damping, the spin angular momentum has to be transferred from the electronic spin system to the lattice, there is no reason why different types of these spin-flip scatterings should be relevant for the two situations. Therefore, the Elliott-Yafet relation, Eq. (2), should be applicable for our system. It would not be valid if nonlocal spin-diffusion processes would contribute a lot to demagnetization. Examples are a superdiffusive spin current in the direction perpendicular to the film plane, or a lateral diffusion out of the spot irradiated by the laser pulse and investigated by the TR-MOKE. However, we definitely found the validity of the Elliott-Yafet relation, and this shows that nonlocal spin-diffusion processes are so small that they can be neglected in our experiment. Furthermore, what we should focus on in this study is the effect of spin precession taking place in ns timescale on the ultrafast demagnetization, whatever the explicit microscopic mechanism of the ultrafast demagnetization.

Despite this, previous demonstrations [17,19–21] show that the ultrafast spin current is caused by the transport of spin-majority and spin-minority electrons in the antiparallel (AP) state of magnetic multilayers after the laser pulse accelerates ultrafast demagnetization. Similarly, as is indicated in Fig. 1(b), with the assistance of an interface between FM

(Ni) and NM (Pt), the spin current induced by the flow of spin-up and spin-down electrons in opposite directions [59] may contribute partly to the Gilbert damping in Pt/Co/Ni/Pt multilayers. The femtosecond laser-induced spin current lives very shortly, in a subpicosecond time scale, while the duration of the spin current triggered by spin precession is in a time scale of nanoseconds. The difference in the duration of the spin current is just related to the time scale of the perturbation of the system. One has to note that spin currents at the femtosecond time scale give rise to a lowering of the demagnetization time [17], while spin-pumping-induced spin current gives rise to the enhancement of Gilbert damping and thus a lowering of the relaxation time. Therefore, when the spin current contributes largely to both ultrafast demagnetization and spin precession dynamics, an inverse relationship between the ultrafast demagnetization time and Gilbert damping could be expected. That is, the more spin current transferred from the ferromagnetic layer to normal metal, the faster the ultrafast demagnetization should be. Therefore, in the present Rapid Communication, explaining the experimental results by using the local Elliott-Yafet scattering theory suffices. Also, the nonlocal spin-current effect can be ignored, although it contributes partly to the fitted value of the spin-mixing parameter b^2 . The discussions here inspire us to continuously clarify the various relationships between ultrafast demagnetization time and Gilbert damping coming from different microscopic mechanisms, which is helpful for understanding the underlying physics of ultrafast spin dynamics as well as the application of ultrafast spin current triggered by ultrashort lasers [60,61]. For instance, recently, researchers have been seeking for potential candidates, such as terahertz wave emitters including metallic heterostructures. Previous demonstrations show that the magnitude and efficiency of terahertz signals in these multilayers are determined by Gilbert damping [60]. The investigations of the relationship between Gilbert damping and ultrafast demagnetization time will open up a different avenue to tailor the terahertz emission.

Meanwhile, the dominant contribution to ultrafast demagnetization in metallic heterostructures, either from localized spin-flip scattering or nonlocal spin transport, has been a controversial issue for a long time [23]. Here, a different approach, by establishing the relation between the demagnetization time and Gilbert damping, is proposed to distinguish the two mechanisms. The proportional relationship indicates the localized spin-flip scattering mechanism dominates, otherwise the nonlocal spin current dominates.

In conclusion, the fast and ultrafast dynamic properties of Ta(3 nm)/Pt(2 nm)/Co(0.8 nm)/Ni(d_{Ni} nm)/Pt(1 nm)/Ta(3 nm) bilayers with the electrons relaxing near the Fermi surface have been investigated by using the TR-MOKE pump-probe technique. A genuine proportional relationship, in contrast to previous trivial consequences induced by an impure mechanism, between ultrafast demagnetization time and the Gilbert damping constant is confirmed from experimental results. The estimated value of the spin-mixing parameter on the basis of the breathing Fermi-surface model is far larger than that of Co or Ni, which originates from the strong spin-orbital coupling at the interface. The successful unification of the ultrafast demagnetization time and Gilbert damping between experiment and theoretical predication is attributed to overcome the rare-earth doping effect in the clean system of Co/Ni bilayer we choose, although the spin-orbit coupling, interfacial hybridization and spin pumping mechanism due to the Pt layer make the system somewhat complicated. It should be taken into account seriously in the future's investigation. More importantly, distinguishing the dominant mechanism underlying ultrafast demagnetization in metallic heterostructures has been a tough task for a long time. Here, an effective method by unifying the ultrafast demagnetization time and Gilbert damping is proposed to solve this task, namely, that a proportional relation between the two parameters indicates the local spin-flip scattering mechanism dominates, otherwise the nonlocal spin-current effect dominates.

This work was supported by the National Basic Research Program of China (973 program, Grants No. 2015CB921403 and No. 2016YFA0300701), the National Natural Sciences Foundation of China (51427801, 11374350, and 91622126). The authors thank Hai-Feng Du, Da-Li Sun, and Qing-feng Zhan for a critical reading and constructive suggestions for the manuscript. The authors are indebted to B. Koopmans and M. Haag for helpful discussions.

Z.H.C. supervised the project. Z.H.C. and W.Z. conceived and designed the experiments. W.Z. and W.H. performed the polar Kerr loops and TR-MOKE measurements. X.Q.Z. made some contributions to the TR-MOKE setup. T.J. provided the samples. M.F. helped with the interpretation of the results on the basis of the breathing Fermi-surface model. All the coauthors contributed to the analysis and discussion for the results. Z.H.C. wrote the paper with input from all the coauthors.

The authors declare no competing financial interests.

-
- [1] E. Beaurepaire, J.-C. Merle, A. Daunois, and J.-Y. Bigot, *Phys. Rev. Lett.* **76**, 4250 (1996).
- [2] A. V. Kimel, A. Kirilyuk, P. A. Usachev, R. V. Pisarev, A. M. Balbashov, and Th. Rasing, *Nature (London)* **435**, 655 (2005).
- [3] E. Turgut, C. La-o-vorakiat, J. M. Shaw, P. Grychtol, H. T. Nembach, D. Rudolf, R. Adam, M. Aeschlimann, C. M. Schneider, T. J. Silva, M. M. Murnane, H. C. Kapteyn, and S. Mathias, *Phys. Rev. Lett.* **110**, 197201 (2013).
- [4] C. Stamm, T. Kachel, N. Pontius, R. Mitzner, T. Quast, K. Holldack, S. Khan, C. Lupulescu, E. F. Aziz, M. Wietstruk, H. A. Durr, and W. Eberhardt, *Nat. Mater.* **6**, 740 (2007).
- [5] A. B. Schmidt, M. Pickel, M. Donath, P. Buczek, A. Ernst, V. P. Zhukov, P. M. Echenique, L. M. Sandratskii, E. V. Chulkov, and M. Weinelt, *Phys. Rev. Lett.* **105**, 197401 (2010).
- [6] B. Koopmans, J. J. M. Ruigrok, F. Dalla Longa, and W. J. M. de Jonge, *Phys. Rev. Lett.* **95**, 267207 (2005).
- [7] B. Koopmans, G. Malinowski, F. Dalla Longa, D. Steiauf, M. Fähnle, T. Roth, M. Cinchetti, and M. Aeschlimann, *Nat. Mater.* **9**, 259 (2010).
- [8] D. Steiauf and M. Fähnle, *Phys. Rev. B* **79**, 140401 (2009).
- [9] C. Illg, M. Haag, and M. Fähnle, *Phys. Rev. B* **88**, 214404 (2013).

- [10] M. Krauß, T. Roth, S. Alebrand, D. Steil, M. Cinchetti, M. Aeschlimann, and H. C. Schneider, *Phys. Rev. B* **80**, 180407 (2009).
- [11] B.-Y. Mueller, M. Haag, and M. Fähnle, *J. Magn. Magn. Mater.* **414**, 14 (2016).
- [12] E. Carpené, E. Mancini, C. Dallera, M. Brenna, E. Puppini, and S. De Silvestri, *Phys. Rev. B* **78**, 174422 (2008).
- [13] M. Haag, C. Illg, and M. Fähnle, *Phys. Rev. B* **90**, 014417 (2014).
- [14] G. P. Zhang and W. Hübner, *Phys. Rev. Lett.* **85**, 3025 (2000).
- [15] G. P. Zhang, M. S. Si, and T. F. George, *J. Appl. Phys.* **117**, 17D706 (2015).
- [16] J.-Y. Bigot, M. Vomir, and E. Beaurepaire, *Nat. Phys.* **5**, 515 (2009).
- [17] G. Malinowski, F. D. Longa, J. H. H. Rietjens, P. V. Paluskar, R. Huijink, H. J. M. Swagten, and B. Koopmans, *Nat. Phys.* **4**, 855 (2008).
- [18] M. Battiato, K. Carva, and P. M. Oppeneer, *Phys. Rev. Lett.* **105**, 027203 (2010).
- [19] A. Eschenlohr, M. Battiato, P. Maldonado, N. Pontius, T. Kachel, K. Holldack, R. Mitzner, A. Föhlisch, P. M. Oppeneer, and C. Stamm, *Nat. Mater.* **12**, 332 (2013).
- [20] D. Rudolf, C. La-O-Vorakiat, B. Battiato, R. Adam, J. M. Shaw, E. Turgut, P. Maldonado, S. Mathias, P. Grychtol, H. T. Nembach, T. J. Silva, M. Aeschlimann, H. C. Kapteyn, M. M. Murnane, C. M. Schneider, and P. M. Oppeneer, *Nat. Commun.* **3**, 1037 (2012).
- [21] W. He, T. Zhu, X.-Q. Zhang, H.-T. Yang, and Z.-H. Cheng, *Sci. Rep.* **3**, 2883 (2013).
- [22] B. Vodungbo, J. Gautier, G. Lambert, A. Barszczak Sardinha, M. Lozano, S. Sebban, M. Ducouso, W. Boutu, K. G. Li, B. Tudu, M. Tortarolo, R. Hawaldar, R. Delaunay, V. López-Flores, J. Arabski, C. Boeglin, H. Merdji, P. Zeitoun, and J. Lüning, *Nat. Commun.* **3**, 999 (2012).
- [23] N. Bergeard, M. Hehn, S. Mangin, G. Lengaigne, F. Montaigne, M. L. M. Laliu, B. Koopmans, and G. Malinowski, *Phys. Rev. Lett.* **117**, 147203 (2016).
- [24] A. J. Schellekens, W. Verhoeven, T. N. Vader, and B. Koopmans, *Appl. Phys. Lett.* **102**, 252408 (2013).
- [25] S. Azzawi, A. Ganguly, M. Tokac, R. M. Rowan-Robinson, J. Sinha, A. T. Hindmarch, A. Barman, and D. Atkinson, *Phys. Rev. B* **93**, 054402 (2016).
- [26] I. Radu, G. Woltersdorf, M. Kiessling, A. Melnikov, U. Bovensiepen, J.-U. Thiele, and C. H. Back, *Phys. Rev. Lett.* **102**, 117201 (2009).
- [27] J. Walowski, G. Muller, M. Djordjevic, M. Munzenberg, M. Klaui, C. A. F. Vaz, and J. A. C. Bland, *Phys. Rev. Lett.* **101**, 237401 (2008).
- [28] Y. Ren, Y. L. Zuo, M. S. Si, Z. Z. Zhang, Q. Y. Jin, and S. M. Zhou, *IEEE Trans. Magn.* **49**, 3159 (2013).
- [29] G. Woltersdorf, M. Kiessling, G. Meyer, J.-U. Thiele, and C.-H. Back, *Phys. Rev. Lett.* **102**, 257602 (2009).
- [30] M. Fähnle and C. Illg, *J. Phys.: Condens. Matter.* **23**, 493201 (2011).
- [31] M. Fähnle, J. Seib, and C. Illg, *Phys. Rev. B* **82**, 144405 (2010).
- [32] S. L. Jiang, X. Chen, X. J. Li, K. Yang, J. Y. Zhang, G. Yang, Y. W. Liu, J. H. Lu, D. W. Wang, J. Teng, and G. H. Yu, *Appl. Phys. Lett.* **107**, 112404 (2015).
- [33] X. Chen, K. Y. Wang, Z. L. Wu, S. L. Jiang, G. Yang, Y. Liu, J. Teng, and G. H. Yu, *Appl. Phys. Lett.* **104**, 052413 (2014).
- [34] See Supplemental Material at <http://link.aps.org/supplemental/10.1103/PhysRevB.96.220415> for more details on the static properties of Co/Ni bilayers, for an understanding of the measurements of spin dynamics in ns time scales and the analysis of extrinsic contributions to spin precession, and for numerical simulations on the effect of heat transport across the film thickness on the ultrafast demagnetization time as well as the table of fitting parameters used in the 3TM model.
- [35] W. He, B. Hu, Q. F. Zhan, X. Q. Zhang, and Z. H. Cheng, *Appl. Phys. Lett.* **104**, 142405 (2014).
- [36] H. S. Song, K. D. Lee, J. W. Sohn, S. H. Yang, Stuart S. P. Parkin, C. Y. You, and S. C. Shin, *Appl. Phys. Lett.* **103**, 022406 (2013).
- [37] S. Mizukami, F. Wu, A. Sakuma, J. Walowski, D. Watanabe, T. Kubota, X. Zhang, H. Naganuma, M. Oogane, Y. Ando, and T. Miyazaki, *Phys. Rev. Lett.* **106**, 117201 (2011).
- [38] H. S. Song, K. D. Lee, J. W. Sohn, S. H. Yang, S. S. P. Parkin, C. Y. You, and S. C. Shin, *Appl. Phys. Lett.* **102**, 102401 (2013).
- [39] T. Kato, Y. Matsumoto, S. Okamoto, N. Kikuchi, O. Kitakami, N. Nishizawa, S. Tsunashima, and S. Iwata, *IEEE Trans. Magn.* **47**, 3036 (2011).
- [40] M. van Kampen, C. Jozsa, J. T. Kohlhepp, P. LeClair, L. Lagae, W. J. M. de Jonge, and B. Koopmans, *Phys. Rev. Lett.* **88**, 227201 (2002).
- [41] Y. Au, M. Dvornik, T. Davison, E. Ahmad, P. S. Keatley, A. Vansteenkiste, B. Van Waeyenberge, and V. V. Kruglyak, *Phys. Rev. Lett.* **110**, 097201 (2013).
- [42] C. Y. Cheng, K. K. Meng, S. F. Li, J. H. Zhao, and T. S. Lai, *Appl. Phys. Lett.* **103**, 232406 (2013).
- [43] Y. Au, T. Davison, E. Ahmad, P. S. Keatley, R. J. Hicken, and V. V. Kruglyak, *Appl. Phys. Lett.* **98**, 122506 (2011).
- [44] B. Lenk, G. Eilers, J. Hamrle, and M. Münzenberg, *Phys. Rev. B* **82**, 134443 (2010).
- [45] G. H. O. Daalderop, P. J. Kelly, and F. J. A. den Broeder, *Phys. Rev. Lett.* **68**, 682 (1992).
- [46] G. Malinowski, K. C. Kuiper, R. Lavrijsen, H. J. M. Swagten, and B. Koopmans, *Appl. Phys. Lett.* **94**, 102501 (2009).
- [47] M. Caminale, A. Ghosh, S. Auffret, U. Ebels, K. Ollefs, F. Wilhelm, A. Rogalev, and W. E. Bailey, *Phys. Rev. B* **94**, 014414 (2016).
- [48] Y. Tserkovnyak, A. Brataas, and G. E. W. Bauer, *Phys. Rev. B* **66**, 224403 (2002).
- [49] Y. Liu, Z. Yuan, R. J. H. Wesselink, A. A. Starikov, and P. J. Kelly, *Phys. Rev. Lett.* **113**, 207202 (2014).
- [50] K. C. Kuiper, G. Malinowski, F. Dalla Longa, and B. Koopmans, *J. Appl. Phys.* **109**, 07D316 (2011).
- [51] K. C. Kuiper, T. Roth, A. J. Schellekens, O. Schmitt, B. Koopmans, M. Cinchetti, and M. Aeschlimann, *Appl. Phys. Lett.* **105**, 202402 (2014).
- [52] S. Iihama, Y. Sasaki, H. Naganuma, M. Oogane, S. Mizukami, and Y. Ando, *J. Phys. D: Appl. Phys.* **49**, 035002 (2016).
- [53] L. I. Berger, Optical properties of selected inorganic and organic solids, in *CRC Handbook of Chemistry and Physics*, 88th ed., edited by D. R. Lide (CRC, Boca Raton, FL, 2007), p. 12-141, 3.1.5, 3.4.
- [54] U. A. Macizo, Modeling of ultrafast laser-induced magnetization dynamics within the Landau-Lifshitz-Bloch approach, Ph.D. thesis, Universidad Autonoma de Madrid, 2012, p. 78.

- [55] B. Vodungbo, B. Tudu, J. Perron, R. Delaunay, L. Müller, M. H. Berntsen, G. Grübel, G. Malinowski, C. Weier, J. Gautier, G. Lambert, P. Zeitoun, C. Gutt, E. Jal, A. H. Reid, P. W. Granitzka, N. Jaouen, G. L. Dakovski, S. Moeller, M. P. Minitti, A. Mitra, S. Carron, B. Pfau, C. von Korff Schmising, M. Schneider, S. Eisebitt, and J. Lüning, *Sci. Rep.* **6**, 18970 (2016).
- [56] F. Dalla Longa, J. T. Kohlhepp, W. J. M. de Jonge, and B. Koopmans, *Phys. Rev. B* **75**, 224431 (2007).
- [57] F. Busse, M. Mansurova, B. Lenk, M. von der Ehe, and M. Münzenberg, *Sci. Rep.* **5**, 12824 (2015).
- [58] K. Gilmore, Y.-U. Idzerda, and M.-D. Stiles, *Phys. Rev. Lett.* **99**, 027204 (2007).
- [59] I. Zutic and H. Dery, *Nat. Mater.* **10**, 647 (2011).
- [60] J. Shen, X. Fan, Z. Y. Chen, M. F. DeCamp, H. W. Zhang, and J. Q. Xiao, *Appl. Phys. Lett.* **101**, 072401 (2012).
- [61] T. Seifert, S. Jaiswal, U. Martens, J. Hannegan, L. Braun, P. Maldonado, F. Freimuth, A. Kronenberg, J. Henrizi, I. Radu, E. Beaurepaire, Y. Mokrousov, P. M. Oppeneer, M. Jourdan, G. Jakob, D. Turchinovich, L. M. M. Hayden, M. Wolf, M. Münzenberg, M. Kläui, and T. Kampfrath, *Nat. Photonics* **10**, 483 (2016).